AVALANCHE DEBRIS DETECTION USING SATELLITE- BORNE RADAR AND OPTICAL REMOTE SENSING

Markus Eckerstorfer[1]*, Eirik Malnes[1], Regula Frauenfelder[2], Ulrik Domaas[2], Kjetil Brattlien[2]

[1]Earth Observation, Norut, Tromsø, Norway
[2]Norwegian Geotechnical Institute, Oslo, Norway

ABSTRACT: The mountainous fjord landscape around Tromsø in Northern Norway is prone to high avalanche activity during the snow season. Large avalanches pose a hazard to infrastructure, such as buildings and roads, located between the steep mountainsides and the fjords. To forecast the spatial and temporal extent of avalanche events, knowledge of past activity is critical. For this, a complete avalanche record is needed, however, difficult to achieve. We hypothesize, that the use of satellite data can assist in mapping avalanches over large areas.
During and shortly after an intense avalanche cycle in the county of Troms in March 2014, we obtained 11 high-resolution Radarsat-2 Ultrafine scenes centered over large observed avalanches, together with one Landsat-8 scene and four Radarsat-2 SCN/SCW scenes with coarser resolution, covering the entire county.
We detected avalanche debris-like features visually, by applying two detection algorithms that make use of the increased backscatter in avalanche debris. This backscatter increase is due to increased snow water equivalent and surface roughness. In addition to the multi-sensor approach using high- to medium-resolution satellite data, we also used a multi-temporal approach. Repeated acquisitions of satellite data from the same area enabled redetection of avalanche debris-like features by change detection methods and, thus, confirmation of their existence.
In this study, we show the usability of satellite radar data in detecting avalanches over a large area with medium resolution. Since ultra-high resolution is not available in an operational context today, our hypothesis based on our results using Radarsat-2 is that the ESA Sentinel-1 satellite could provide sufficient coverage and resolution to detect medium and large sized avalanches.

KEYWORDS: avalanche debris detection, radar remote sensing, Radarsat-2

1. INTRODUCTION

Avalanche warning centers worldwide work towards minimizing the number of fatal backcountry avalanche accidents, while road and railroad authorities work towards securing their infrastructure and passengers against destruction from large, spontaneous avalanches.

One crucial part in basic avalanche hazard assessment and warning is the knowledge of avalanche activity in space and time in a given region. It is controlled by meteorology and snowpack as the dynamic factors, and topography as the static factor (Schweizer et al., 2003a). The goal for responsible authorities is the collection of a complete, long-term dataset of avalanche activity and its characteristics (Haegeli and McClung, 2003). Such so-called avalanche climate classifications exist from many mountain areas worldwide (Armstrong and Armstrong, 1987; Baggi and Schweizer, 2009; Mock and Birkeland, 2000). These datasets are used for a wide range of applications, spanning from statistical avalanche forecasting (Hendrikx et al., 2014), to return-period calculations (Eckert et al., 2010) and climate change studies (Marty and Meister, 2012).

The largest uncertainty in these avalanche activity datasets is the lack of completeness. Avalanches occur in inaccessible mountain terrain, making it difficult to observe all activity. This leads to an incomplete record, as well as uncertainty in the exact release timing, resulting in poor correlations with triggering factors (Schweizer et al., 2003b).

2. SCOPE OF THE STUDY

In our view, data gaps in incomplete avalanche records could be filled by using satellite remote sensing in order to detect avalanches over large,

* *Corresponding author address:*
Markus Eckerstorfer, Earth Observation, Norut
P.O. Box 6434, Tromsø Science Park, 9294 Tromsø, Norway;
tel: +47 92678797;
email: markus.eckerstorfer@norut.no

inaccessible areas. Studies on space-borne avalanche detection are to date sparse. A few studies showed the potential to detect avalanches using optical sensors (Bühler et al., 2009; Bühler et al., 2013; Lato et al., 2012). The use of synthetic aperture radar (SAR) remote sensing in avalanche detection was first shown by Wiesmann et al. (2001). The authors used the high backscatter of rough, compacted avalanche debris-snow from ERS1/2 data to discriminate avalanche debris from the surrounding snow surface. More recently, Malnes et al. (2013) used multi-temporal processing of Radarsat-2 scenes (3x3 m) to detect large avalanches in Northern Norway. Radar data, such as Synthetic Aperture Radar (SAR) has the advantage of being unaffected by light and cloud conditions.

We, thus, hypothesize that the use of multi-temporal and multi-sensor, satellite-borne SAR remote sensing can assist in systematically mapping avalanche activity.

To test our hypothesis, we collected 11 Radarsat-2 Ultrafine scenes (RS-2 U), 2 Radarsat-2 ScanSAR narrow (RS-2 SCN), and 2 Radarsat-2 Scan wide (RS-2 SCW) scenes during March 2014 covering parts of the county Troms in Northern Norway.

3. METHODS

3.1 Satellite-data acquisition, processing and analysis

All RS-2 scenes were either ordered after large avalanches or when high avalanche activity in a certain area was reported. Eleven RS-2 U scenes covered seven individual areas, with four areas covered by at least two scenes. Thus a total area of about 2800 km^2 was covered.

All RS-2 scenes (Tbl. 1) were geocoded with Norut's' software GSAR (Larsen et al., 2005) using a 10 m digital terrain model. Multi-looking was applied to suppress speckle noise.

Two avalanche debris detection algorithms were applied:

1) Single image detection, which involves simple image enhancement methods to improve the backscatter contrast between avalanche debris and the surrounding snow surface. The increased backscatter of avalanche debris is due to increased snow water equivalent, snow depth and surface roughness. Distinct avalanche debris-like features were visually mapped in ArcGIS10.

2) Dual-pole detection, which makes use of the different polarizations (HH, HV or VH, VV) in SAR data. The algorithm produces color red-green-blue (RGB) images, where different polarizations were assigned to different channels in the RGB image. The typical tongue shapes of avalanches appear with an enhanced color signature in the RGB-image.

The Landsat-8 (LS-8) scenes, as well as field photographs (example given in Fig. 1), were used as auxiliary data to validate and confirm the radar image analysis.

Tbl. 1: Acquired satellite data

#	*Type*	*Swath (km)*	*Resolution (m)*
11	RS-2 U	20x20	3x3
2	RS-2 SCW	500x500	100x100
2	RS-2 SCN	300x300	50x50
2	LS-8	185x185	15x15

3.2 Topographic GIS modelling

In order to roughly distinguish between highly probable avalanche terrain and areas where the occurrence of avalanche releases are unlikely (even though not impossible) a simple topographic GIS model was used (Bühler et al., 2013). We applied the GIS model after the detection of avalanche debris-like features.

For each detected feature we tested if (1) the starting zone inclination was steeper than 35° (the starting zone was defined as the general area in the fall line above any avalanche debris-like feature; fall lines for each feature were calculated in GIS) and if (2) the runout zone had a slope inclination of less than 25° (the runout zone was defined as the area around the point of the furthest downslope position of the avalanche debris-like feature).

If both topographic conditions were given, the avalanche debris-like features were classified as avalanche debris.

4. RESULTS

4.1 The avalanche cycle of March 2014

In the county of Troms high avalanche activity in the earlier parts of the winter 2013/14 was followed by a considerably calm phase during January and February. Enhanced polar low activity

starting in the beginning of March resulted in high avalanche activity during the entire month. Avalanche releases were mainly caused by three factors: a) releases due to bad bonding between different layers of recent storm snow, resulting in medium avalanches, b) bad bonding at the interface between old- and new snow, resulting in large avalanches, c) releases due to rain-on-snow events both in the beginning and the end of March, resulting in large wet slab avalanches (Landrø et al., 2013). Some of these destructive size 4 avalanches buried roads (Fig. 1)

4.2 Avalanche debris detection

In Fig. 2, we show an example of avalanche debris-like feature detection in a RS-2 U scene, using the single image detection algorithm. Elongated, tongue-shaped features with an increased backscatter signature are clearly visible. Our interpretation is shown in Fig. 2b. The topographic GIS model (Fig. 2c) helps to distinguish actual avalanche debris from features that mistakenly might be regarded as avalanche debris, such as radar artifacts, areas with topographic foreshortening, and radar shadows.

Fig. 1: Avalanche path crossing the E6 between Hatteng and Storfjord. On 11 March 2014, the road was blocked twice due to avalanches from this avalanche path. (Image courtesy: above) Kjetil Brattlien, NGI; below) Dan Henrik Klausen, NRK). This avalanche could be mapped in the RS-2 U scene from 15 March 2014 (red footprint in Fig. 4).

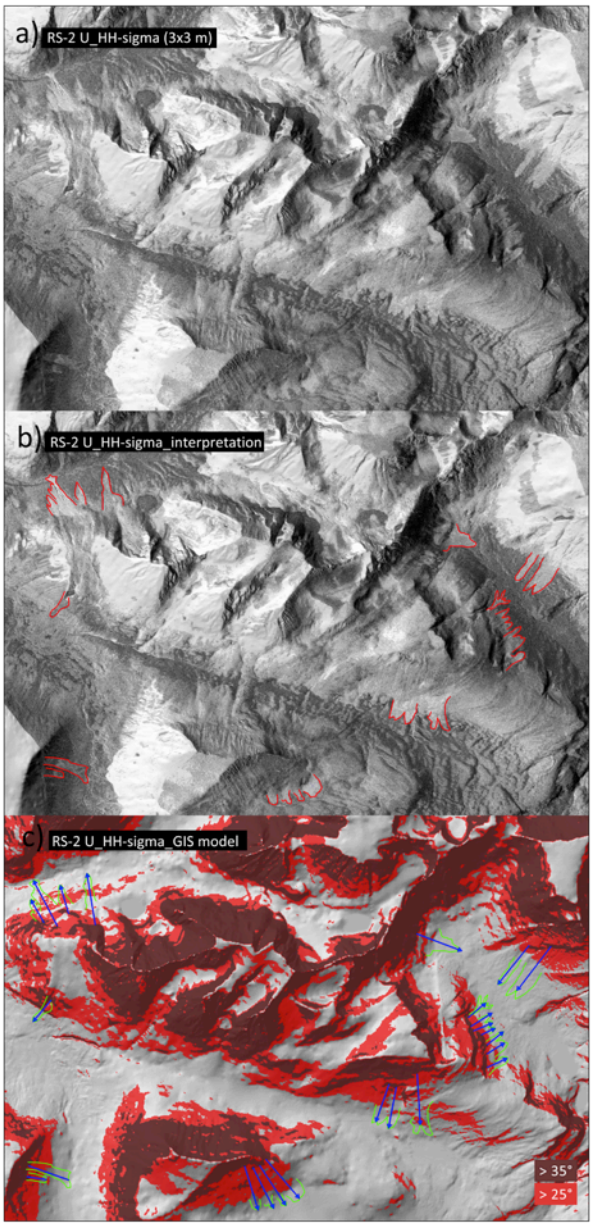

Fig. 2: Single image detection algorithm applied to a RS-2 U scene from 23 March 2014: a) SAR backscatter image with visible avalanche debris-like features, i.e. areas with an increased backscatter signature as compared to their surrounding; b) Visual interpretation of the backscatter signature, suspected avalanches marked with red outlines; c) Visual representation of the topographic GIS model with dark red areas depicting probable starting zones, and

red areas depicting areas below the starting zone, steeper than 25°. The blue arrows indicate the fall lines between the starting zone and the furthest downslope position of the avalanche debris-like feature.

We acquired multiple radar scenes and optical scenes over similar areas. This enabled us to apply a multi-temporal and multi-sensor analysis of initially mapped avalanche debris. In Fig. 3a, three avalanche debris-like features were mapped already in mid-February 2014, based on the enhanced contrast of the cross-polarization image in a 100 x 100 m RS-2 SCN scene. One month later, (Fig. 3b) these features were still visible (captured in a LS-8 scene), however, only as two features. In the green and red boxes, two individual avalanche debris-like features were redetectable one week later in a high-resolution RS-2 U image (Fig. 3c), as well as in a low-resolution RS-2 SCW image (Fig. 3d). Various other avalanches were discernable in both the LS-8 and the RS-2 SCW data. This example is from the valley Lavangsdalen featuring a busy road affected by frequent avalanche activity. It shows that, with some constraints, avalanches can even be detected in low-resolution radar scenes. The multi-sensor and multi-temporal approach helps to capture a more complete avalanche activity record.

In a study area of about 2800-km^2 (roughly 70 x 40 km), we detected 546 avalanche debris-like features in imagery from March 2014 (Fig. 3). The topographic GIS model eliminated fifteen of these features. From the remaining 531 features, 57 were counted multiple times as they reappeared in several radar scenes. The elimination of these multiple counts resulted in a total count of 467 features that we interpret to be avalanche debris. The majority of the detections with 212 avalanches were done in three RS-2 U scenes from 23 and 25 March. These scenes were captured after a phase with intense low-pressure activity, with air temperatures above the freezing point and heavy rain.

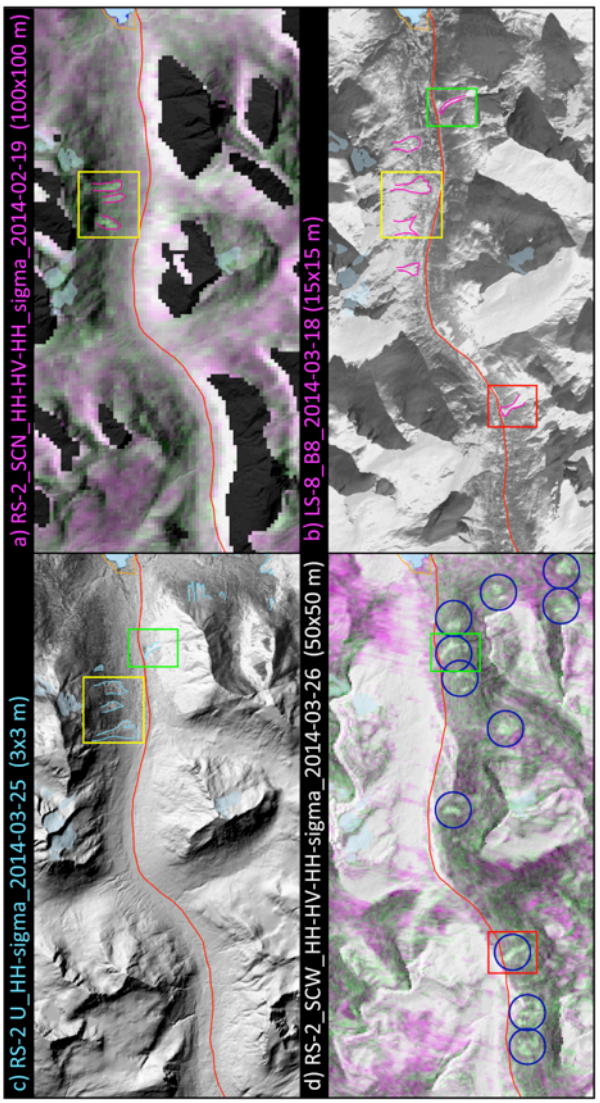

Fig. 3: Multi-temporal and multi-sensor avalanche debris detection: a) RS-2 SCN RGB image (100 x 100 m) with cross polarization. Three avalanche debris-like features appear in light green (purple outlines within yellow box); b) LS-8 scene (15 x 15 m) with avalanche features outlined in purple. The initially mapped features are still visible, however, as two avalanches as opposed to three features in a). The features in the green and red boxes reappear in later scenes; c) RS-2 U scene were avalanche features are mapped in light blue, the three initial avalanches (in yellow box) are still visible; d) RS-2 SCW RGB image (50 x 50 m) with cross polarization. Avalanches (encircled in blue) appear in light green.

5. DISCUSSION

5.1 Multi-temporal and multi-sensor detection of avalanche debris

During March 2014, we acquired 11 RS-2 scenes from seven individual locations. We acquired RS-2 scenes from the same location (partly to fully overlapping) sometimes multiple times, with a minimum of one day and a maximum of 25 days between scenes. Of 467 detected avalanches, 57 avalanches could be redetected in a later scene (with different geometry) confirming, with high confidence, the feature to be an avalanche. This multi-temporal analysis excluded the possibility that these features could be radar artifacts. However, avalanches could not be redetected when the return period of a scene was 25 days, probably due to the removal of the avalanche debris signature by new snow and/or wind. A more consistent acquisition of SAR data, with small temporal baselines over the same area is of critical importance for the successful establishment of complete avalanche records.

We could partly eliminate this problem by using a multi-sensor approach that significantly improved the long-term redetection of avalanche debris. By using different sensors, we have shown that avalanches were consistently detectable over time. We observe, however, a change in the mapped outlines due to the different sensor resolutions and differences in sensor geometries (Fig. 3).

5.2 Sensor performances in detecting avalanche debris

RS-2 U scenes with a pixel resolution of 3 m were obviously best suited for avalanche debris detection. The smallest avalanche debris detected had a cross-slope width of 45 m. A repeated acquisition of RS-2 U scenes from the same region makes this approach a stand-alone methodology. However, RS-2 U scenes are costly, availability is not consistent and the swath is small. Furthermore, layover and shadow effects often affect large parts of the scenes, especially in steep terrain.

Various reports from local informants (such as police, road maintenance personnel, residents) about observed avalanches helped to confirm many of our findings. In addition, freely available LS-8 scenes with a pixel resolution of 15 m were to some degree usable for avalanche debris detection. The swath of a LS-8 scene is large, however, cloud cover and shadows are a problem.

5.3 Topographic GIS model

The simple topographic GIS model assisted in the detection of avalanche debris by depicting steep enough starting zone inclinations and low-angled furthest runout locations. The used approach is obviously an oversimplification, however, helpful in eliminating complete misinterpretations due to radar artifacts, topographic foreshortening, and radar shadows. The GIS model is largely dependent on the DEM resolution, which if too coarse, can add uncertainties to the slope angle calculations.

6. CONCLUSIONS AND OUTLOOK

In March 2014, an intense avalanche cycle in the county of Troms caused numerous road closures and culminated in one avalanche fatality. To forecast such cycles, their spatial extent and magnitude, knowledge of past avalanche activity is an important prerequisite. Complete avalanche records for a given forecasting area would be a major step forward.

Satellite-borne SAR detection of avalanche debris could help filling this gap. In this study, we have shown that avalanche activity can be mapped using a multi-sensor and multi-temporal approach. SAR scenes are ideal for such a task, as they are independent of cloud cover and light conditions.

We would like to note that the goal of this study was not to detect the full extent of the March 2014 avalanche cycle in the county of Troms. The overall goal of this study was to improve avalanche debris detection methods based on single case studies. Therefore, the acquired satellite data may seem inconsistent in space and time.

Currently, we are working on the automated detection of avalanche debris, based on backscatter differences, since the visual inspection done in this study is too time consuming.

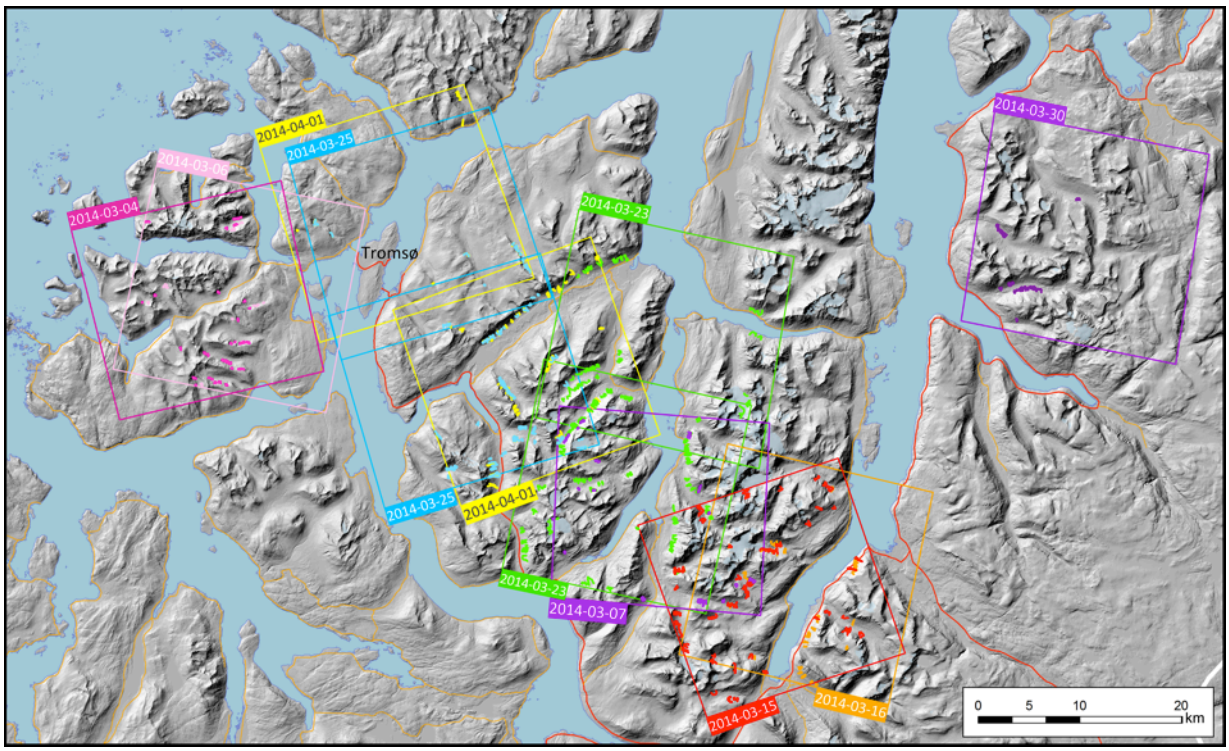

Fig. 4: Topographic map of the county of Troms. The colored frames depict the swath of RS-2 U scenes, collected during March 2014. The accordingly colored tongue-shaped features are detected avalanche debris (n = 546, incl. 57 multiple counts). Both the RS-2 SCW and SCN and the LS-8 scenes (footprints not shown here) cover the entire mapped area. Background: DEM from Norwegian Mapping Authority (Statens Kartverk).

The requirements for creating a complete avalanche activity record could be fulfilled using Sentinel-1 scenes, which will be available with a worldwide coverage from autumn 2014 .The Sentinel-1 satellite(s) will deliver high-resolution SAR data, with a large swath (250x250 km) and a short repeat time (12 days at mid-latitudes, down to 3 days at northern latitudes). The acquisition of Sentinel-1 scenes, together with automated avalanche debris detection and application of a topographic GIS model could make it feasible to compile a complete avalanche activity database for a given area. This could be a first step towards the operational use of SAR remote sensing data in avalanche forecasting.

ACKNOWLEDGEMENTS

This work has been financed by the Center for remote sensing of avalanches (SeFaS), and the ESA PRODEX project ASAM ("Towards an automated snow property and avalanche mapping system"), contracts 4000107724/-664/-694/-722.

Radarsat-2 data has been acquired on a quota from the Norwegian Radarsat-2 agreement, copyright @ MDA/NSC/KSAT (2014). Landsat-8: Image courtesy of the U.S. Geological Survey, 2014.

We used a digital elevation model from the Norwegian Mapping Authority (Statens Kartverk).

The reconnaissance flights have been carried out within NGIs assignment during Nato's Cold Response 2014 exercise.

REFERENCES

Greene, E., T. Wiesinger, K. W. Birkeland, C. Coleou, A. Jones, and G. Statham, 2006: Fatal avalanche accidents and forecasted danger levels: Patterns in the United States, Canada, Switzerland and France. Proceedings of the *International Snow Science Workshop*, Telluride, CO, 640-649.

McClung, D. M. and P. A. Schaerer, 2006: *The Avalanche Handbook*. 3rd ed. The Mountaineers, 347 pp.

Schweizer, J. and J. B. Jamieson, 2003: Snowpack properties for snow profile analysis. *Cold Regions Science and Technology*, 37, 233-241.Armstrong, L.R. and Armstrong, B.R., 1987. Snow and avalanche climates of the western United States: A comparison of maritime, intermountain and continental conditions. Proceedings of the Davos Symposium, IAHS Publ., 162: 281-294.

Baggi, S. and Schweizer, J., 2009. Characteristics of wet-snow avalanche activity: 20 years of observations from a high alpine valley (Dischma, Switzerland). Natural Hazards, 50(1): 97-108.

Bühler, Y., Hüni, A., Christen, M., Meister, R. and Kellenberger, T., 2009. Automated detection and mapping of avalanche deposits using airborne optical remote sensing data. Cold Regions Science and Technology, 57(2–3): 99-106.

Bühler, Y., Kumar, S., Veitinger, J., Christen, M., Stoffel, A. and Snehmani, 2013. Automated identification of potential snow avalanche release areas based on digital elevation models. Nat. Hazards Earth Syst. Sci., 13: 1321-1335.

Eckert, N., Coleou, C., Castebrunet, H., Dechatres, M., Giraud, G. and Gaume, J., 2010. Cross-comparison of meteorological and avalanche data for characterising avalanche cycles: The example of December 2008 in the eastern part of the French Alps. Cold Regions Science and Technology, In Press, Corrected Proof.

Haegeli, P. and McClung, D.M., 2003. Avalanche characteristics of a transitional snow climate--Columbia Mountains, British Columbia, Canada. Cold Regions Science and Technology, 37(3): 255-276.

Hendrikx, J., Murphy, M. and Onslow, T., 2014. Classification trees as a tool for operational avalanche forecasting on the Seward Highway, Alaska. Cold Regions Science and Technology, 97: 113-120.

Landrø, M., Kosberg, S. and Müller, K., 2013. Avalanche problems; an important part of the Norwegian forecast, and a ueful tool for the users, Proceedings of the International Snow Science Workshop 2013, Grenoble - Chamonix Mont-Blanc.

Larsen, Y., Engen, G., Lauknes, T.R., Malnes, E. and Høgda, K.A., 2005. A generic differential interferometric SAR processing system, with applications to land

subsidence and snow-water equivalent retrieval. In: E. ESRIN (Editor), Fringe ATSR Workshop 2005, Frascati, Italy, pp. 6.

Lato, M.J., Frauenfelder, R. and Bühler, Y., 2012. Automated detection of snow avalanche deposits: segmentation and classification of optical remote sensing imagery. Nat. Hazards Earth Syst. Sci., 12(9): 2893-2906.

Malnes, E., Eckerstorfer, M., Larsen, Y., Frauenfelder, R., Jonsson, A., Jaedicke, C. and Solbø, S.A., 2013. Remote sensing of avalanches in northern Norway using Synthetic Aperture Radar, Proceedings of the International Snow Science Workshop 2013, Grenoble - Chamonix, Mont Blanc, France, pp. 955-959.

Marty, C. and Meister, R., 2012. Long-term snow and weather observations at Weissfluhjoch and its relation to other high-altitude observatories in the Alps. Theoretical and Applied Climatology.

Mock, C.J. and Birkeland, K.W., 2000. Snow Avalanche Climatology of the Western United States Mountain Ranges. Bulletin of the American Meteorological Society, 81(10): 2367-2392.

Schweizer, J., Jamieson, B.J. and Schneebeli, M., 2003a. Snow avalanche formation. Reviews of Geophysics, 41(4): 1-25.

Schweizer, J., Kronholm, K. and Wiesinger, T., 2003b. Verification of regional snowpack stability and avalanche danger. Cold Regions Science and Technology, 37(3): 277-288.

Wiesmann, A., Wegmueller, U., Honikel, M., Strozzi, T. and Werner, C.L., 2001. Potential and methodology of satellite based SAR for hazard mapping., IGARSS 2001. IEEE, Sydney, Australia.